JOURNAL OF SOLID STATE CHEMISTRY **84**, 102–117 (1990)

A Study of the Decomposition of Neodymium Hydroxy Carbonate and Neodymium Carbonate Hydrate

HIROFUMI HINODE, RENU SHARMA,* AND LEROY EYRING

*Department of Chemistry and *Center for Solid State Science, Arizona State University, Tempe, Arizona 85287-1604*

Received June 7, 1989; in revised form September 18, 1989

Comprehensive studies of the decomposition of $(NdOH)CO_3$ and $Nd_2(CO_3)_3 \cdot 8H_2O$ have been carried out. The atomic level details of the decomposition as revealed by high-resolution electron microscopy are correlated with the results from thermogravimetric analysis and high-temperature X-ray diffraction analysis. The two sequences of decomposition are found to be

$$(NdOH)CO_3 \rightarrow (NdO)_2CO_3\text{-I} + (NdO)_2CO_3\text{-II} \rightarrow (NdO)_2CO_3\text{-II} \rightarrow (NdO)_2CO_3\text{-II} + Nd_2O_3\text{-A} \rightarrow Nd_2O_3\text{-A} + Nd_2O_3\text{-C} \rightarrow Nd_2O_3\text{-A}$$

and

$$Nd_2(CO_3)_3 \cdot 8H_2O \rightarrow Nd_2(CO_3)_3 \cdot H_2O \rightarrow Nd_2(CO_3)_3 \rightarrow (NdO)_2CO_3\text{-I} \rightarrow (NdO)_2CO_3\text{-I} + (NdO)_2CO_3\text{-II} \rightarrow (NdO)_2CO_3\text{-II} + (NdO)_2CO_3\text{-I} + Nd_2O_3\text{-C} \rightarrow Nd_2O_3\text{-A} + Nd_2O_3\text{-C}.$$

Introduction

Rare-earth oxides have received much attention in the past decade or two, partly because of new applications of these materials both as matrices and dopants in catalyst support, electrical, optical, magnetic, nuclear, and superconducting technologies.

The carbonates of the rare-earth metals, like their oxalates, are used in the preparation of rare-earth-containing oxides. The thermal decomposition of rare-earth carbonates has been the subject of numerous studies (*1–6*). A large spread of the reported decomposition conditions of the intermediate compounds has been reported.

The particular strength of electron microscopic techniques applied here in the study of the thermal decomposition lies in the observation of the *in situ* dynamical process. An electron microscopic investigation of neodymium hydroxycarbonate (β-$NdOHCO_3$) has been carried out by H. Dexpert *et al.* using a JEOL 100C electron microscope (*7, 8*). They reported that the transition was topotactic and they established the crystallographic orientations between the hydroxycarbonate and the product dioxymonocarbonate:

$$\beta\text{-}NdOHCO_3 \rightarrow (NdO)_2CO_3\text{-II} \rightarrow Nd_2O_3\text{-A}.$$

This sequence of reactions is realized in this series of layered hexagonal compounds. Dexpert *et al.* found two different epitaxial relationships with the initial hy-

0022-4596/90 $3.00

droxycarbonate matrix. In one, the *c*-axes of the hexagonal structures are common, and the [1,1,0] of $NdOHCO_3$ and the [0,1,0] of the dioxycarbonate are parallel, and in the other, the two *c*-axes are distinct but parallel. They could not determine the epitaxial condition of the decomposition of the dioxycarbonate to the oxide.

In the present study the thermal decomposition process of neodymium hydroxycarbonate (α-$NdOHCO_3$) and neodymium carbonate hydrate ($Nd_2(CO_3)_3 \cdot 8H_2O$) through intermediate compounds to the sesquioxide (Nd_2O_3) were investigated. Thermogravimetric techniques, room-temperature powder X-ray diffraction methods and high-temperature X-ray diffraction methods were used to map out the macroscopic features of the decomposition. High-resolution electron microscopy (HREM) was used to observe the atomic-level reaction process.

Sample Preparation

The neodymium carbonate hydrate ($Nd_2(CO_3)_3 \cdot 8H_2O$) was prepared by dissolving the oxide (Nd_2O_3, 99.999%) in an aqueous solution containing a slight excess of 25% trichloracetic acid with subsequent heating to decompose the trichloroacetate ion (*1*, *9*):

$$2Nd(C_2Cl_3O_2)_3 + 3H_2O \rightarrow Nd_2(CO_3)_3 + 6CHCl_3 + 3CO_2.$$

The starting solution was prepared by dissolving about 5 g of the oxide in 130 ml of the trichloracetic acid solution, heating until precipitation started, cooling, adding crystals of trichloracetic acid until the precipitate just dissolved, and then diluting to 150 ml.

The decomposition of the trichloroacetate solution was accomplished by bubbling CO_2 through it at 80–90°C for about 20 min. The carbonate was filtered by suction and washed thoroughly with ethanol and then water until the washings were free from chloride as established by the Beilstein test ($Ag + Cl \rightarrow AgCl \downarrow$), then again with ethanol, and finally with ethyl ether in order to hasten drying.

The neodymium hydroxycarbonate ($NdOHCO_3$) was prepared by using the filtered solution containing neodymium trichloroacetate described above. The filtrate was heated at 80–90°C for about 2 hr without bubbling CO_2. This precipitate was treated in the same way as the hydrate.

The neodymium carbonate anhydrate ($Nd_2(CO_3)_3$) was prepared from the octahydrate by heating the latter at about 350°C for 70 hr.

Experimental Procedures

(*1*) *The Thermogravimetric Study*

Thermal decomposition in air was accomplished using a CAHN 1000 electrobalance. The weighed sample of about 40–90 mg was suspended in a platinum bucket at the end of a Pt wire. During thermogravimetric analysis, the sample temperature was continuously raised 15°C/hr from room temperature to 900°C. The temperature and weight were recorded simultaneously.

In separate experiments specimens for room-temperature X-ray identification were prepared as follows. The furnace was heated at the desired temperature for about 2–3 hr. After the temperature reached a constant value, the furnace was raised, and thereby the reaction was started. The weight change and the temperature of the sample were simultaneously recorded on a chart as a function of time. The furnace was lowered after the weight was judged to have attained a constant value. The furnace was then set to the next desired temperature, and the procedure repeated. These annealed specimens were considered to be near equilibrium.

TABLE I

JCPDS Cards Used for Compound Identification

α-$NdOHCO_3$	27-1296	$Nd_2(CO_3)_38H_2O$	31-877
$(NdO)_2CO_3$-I	25-567	$Nd_2(CO_3)_3H_2O$	28-670
$(NdO)_2CO_3$-IA	23-421	Nd_2O_3-A	6-408
$(NdO)_2CO_3$-II	37-806	Nd_2O_3-C	21-579

(2) *The Room-Temperature Powder X-ray Diffraction Study*

X-ray diffraction patterns of the samples cooled to room temperature were obtained with a diffractometer using monochromatized Cu$K\alpha$ radiation (Geigerflex D/max B, Rigaku Co.).

(3) *The High-Temperature X-ray Diffraction Study*

A high-temperature X-ray diffractometer attachment (D2311B1, Rigaku Co.) was used for the observation of *in situ* decomposition of carbonate compounds. The Geigerflex D/max-RB X-ray diffractometer system (rotating anode type, RV-200B, Rigaku Co.) was adopted for the X-ray studies. The powdered sample was ground in an agate mortar with propyl alcohol to a paste. It was then applied to the sample plate made of Pt and the surface made flat by pressing. The sample was heated at about 5°C/min to the desired temperature, and the diffraction pattern was taken after waiting about 60–240 min.

(4) *The High-Resolution Electron Microscopic Study*

For the HREM studies, samples were crushed and suspended in alcohol to obtain a distribution of fine particles. A drop of this suspension was placed on a holey carbon film supported on a copper grid. For microscopic analysis, JEOL 200CX and JEOL 4000EX microscopes equipped with top-entry double-tilt goniometers, operating at 200 and 400 kV, respectively, were used.

Optical diffraction measurements were made from the HREM micrographs using a monochromatic laser beam source mounted on an optical bench.

Identification of the compounds formed was made by comparison of *d*-spacings with the JCPDS cards listed in Table I.

Results and Discussion

(1) *Thermogravimetric Analysis and Room-Temperature Powder X-ray Diffraction Studies*

Figures 1 and 2 record the thermal decomposition of α-$NdOHCO_3$ and $Nd_2(CO_3)_3 \cdot 8H_2O$, respectively, during thermogravimetric runs (continuous curves) showing the sequential ranges of stability of the intermediates during reaction. The final products were identified as A-type Nd_2O_3 by X-ray diffraction. Furthermore, some of the samples of equilibrated intermediate phases cooled from the preparation temperatures were identified by powder X-ray diffraction. The preparative temperatures are shown and the structures identified in Fig. 1 (symbols ▲, ■, ▼, ◆) and in Fig. 2 (■, ▼, ◇, ○, △, □). Filled circles (●) indicate other equilibration runs.

Samples from Run Numbers 4 and 8 were identified as monoclinic $(NdO)_2CO_3$-IA (type-IA), and Run Number 12 was identified as tetragonal $(NdO)_2CO_3$-I (type-I). The transformation of I to IA was reported by J. O. Sawyer *et al.* (*10*) as was the transformation of $(NdO)_2CO_3$-IA to the hexagonal $(NdO)_2CO_3$-II (type-II). However, these transformations were not observed in these experiments. $(NdO)_2CO_3$ was observed to decompose directly to Nd_2O_3 and the reported intermediate phase $Nd_2O_3 \cdot 0.75CO_2$ (*1*) was not found.

The decomposition temperatures listed in Table II were taken as the point at which

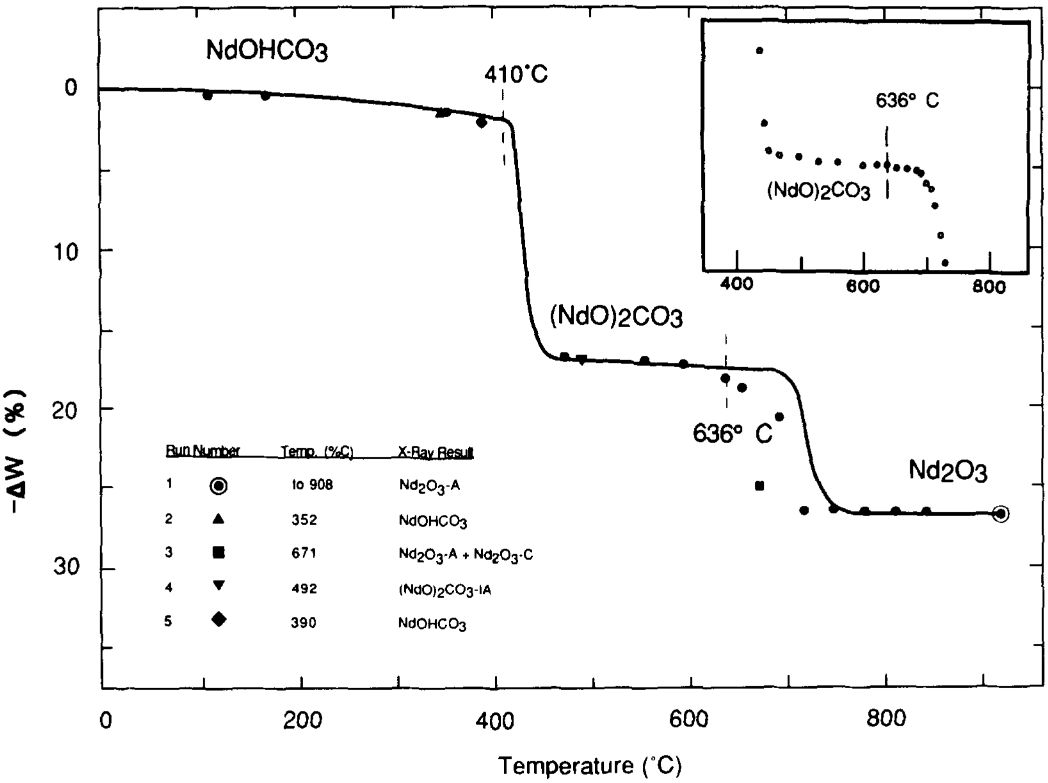

FIG. 1. Thermogravimetric observations on α-$NdOHCO_3$. The solid line is from continuous heating at 15°C/hr. Symbols mark "equilibrium" points from which room-temperature powder diffraction patterns indicated the phases present as marked in the inset at bottom left. Dashed lines mark decomposition temperatures. The inset at the upper right shows in detail the basis of 636°C as the decomposition temperature of $(NdO)_2CO_3$.

TABLE II

THE DECOMPOSITION TEMPERATURES OF $NdOHCO_3$ AND $Nd_2(CO_3)_3 \cdot 8H_2O$, THEIR INTERMEDIATE PRODUCTS, AND THE RESULTS OF X-RAY ANALYSIS

	$(NdOH)CO_3 \rightarrow$	$(NdO)_2CO_3 \rightarrow$	Nd_2O_3	Heating rate/ atmosphere
Present study	410°C	636°C		0.25°C/min/air
Akinc and Sordelet (*2*)	510	735		20°C/min/air
	$Nd_2(CO_3)_3 \cdot 8H_2O \rightarrow$	$Nd_2(CO_3)_3 \rightarrow$	$(NdO)_2CO_3 \rightarrow Nd_2O_3$	
Present study	50,90°C	395°C	620°C	0.25°C/min/air
Head and Holley (*1*)	58	406	620	0.6°C/min/20 Torr H_2O
Sastry *et al.* (*3*)	340	520	820	3–5°C/min/air
Wendlandt and George (*4*)	120	525	785	5°C/min/air
Charles (*5*)		400	580	2°C/min/argon
Cheng and Yen (*6*)	140	370	550	5°C/min/air

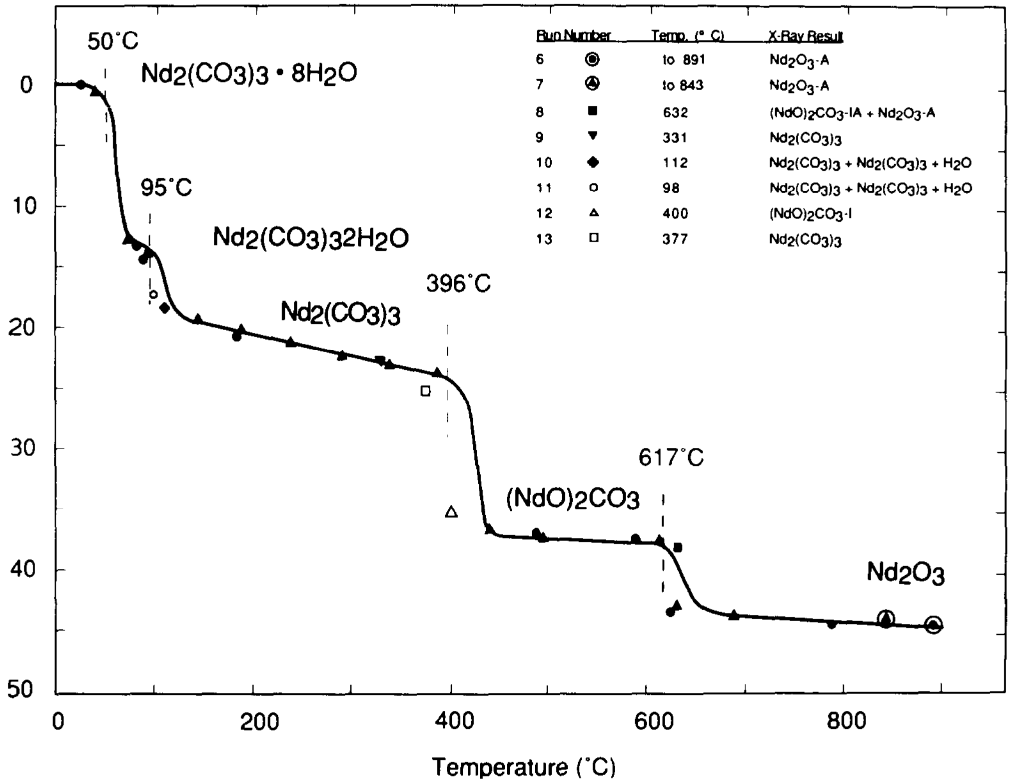

FIG. 2. Thermogravimetric observations on $Nd_2(CO_3)_3 \cdot 8H_2O$. The solid line is from continuous heating at 15°C/hr. Symbols mark "equilibrium" points from which room-temperature powder diffraction patterns indicted the phases present as marked in the inset at the upper right. Dashed lines mark decomposition temperatures.

the continuous TGA curve deviates below a straight line in each intermediate phase region. The decomposition temperatures of $NdOHCO_3$ and $(NdO)_2CO_3$ observed in this study were significantly lower than those observed by Akinc (*2*). The probable reason is that the specimen heating rates differed by almost an order of magnitude. The decomposition temperatures of the present study of $Nd_2(CO_3)_3 \cdot 8H_2O$ are similar to those of Head (*1*) but much lower than those of Sastry (*3*) or Wendlandt (*4*). The differences with the latter two could be due to a combination of much lower heating rates and the method of choosing the decomposition temperature. The start of dehydration of the octahydrate would be the most sensitive to the differences of atmosphere and heating rates. The lower decomposition temperature of the $(NdO)_2CO_3$ in argon as observed by Charles (*5*) is possibly due to the atmosphere and the choice of the initiation temperature. Cheng's results (*6*) are not easily rationalized.

The apparent difference in the decomposition temperatures of $(NdO)_2CO_3$ and the shape of the TGA curves, depending on whether the dioxymonocarbonate source is the hydroxycarbonate or the carbonate, is due to the polymorphism of the $(NdO)_2CO_3$ (type-I or -II) as is clearly shown in the next section. It must be emphasized that the criteria for assessing the onset of decomposition is different and somewhat subjective in each method, hence, all things considered, a wide variation should be expected.

(2) *The High-Temperature X-ray Diffraction Studies*

The *in situ* observation of the decomposition processes and phase reactions of neodymium hydroxycarbonate (α-$NdOHCO_3$), the carbonate hydrate ($(Nd_2CO_3)_3 \cdot 8H_2O$), and the carbonate ($Nd_2(CO_3)_3$) were made using high-temperature X-ray diffraction. Figure 3 shows typical results of the successive changes observed for (a) $NdOHCO_3$ and (b) $Nd_2(CO_3)_3 \cdot 8H_2O$. These results are interpreted and summarized in Table III. The carbonate octahydrate and the carbonate anhydrate gave the same results.

Contrary to the results obtained in the powder X-ray diffraction of cooled specimens, no evidence for the monoclinic $(NdO)_2CO_3$-IA was found in the high-temperature X-ray studies. This is in agreement with Turcotte *et al.* (*11*) who did not observe the type-IA in their high-temperature X-ray studies. Type-IA may be a low-temperature form which is not involved in the thermal decomposition process itself.

(a) From the high-temperature X-ray studies an apparent decomposition route of $NdOHCO_3$ is as follows:

$$NdOHCO_3 \rightarrow (NdO)_2CO_3\text{-I} + (NdO)_2CO_3\text{-II} \rightarrow (NdO)_2CO_3\text{-II} \rightarrow (NdO)_2CO_3\text{-II} + Nd_2O_3\text{-A} \rightarrow Nd_2O_3\text{-A} + Nd_2O_3\text{-C} \rightarrow Nd_2O_3\text{-A}.$$

TABLE III

THE RESULTS FROM HIGH-TEMPERATURE X-RAY OBSERVATIONS OF THE DECOMPOSITION OF $NdOHCO_3$

(1) $NdOHCO_3$		$NdOHCO_3$
	430°C	$(NdO)_2CO_3$(-I) + $(NdO)_2CO_3$(-II)
	600	$(NdO)_2CO_3$-II
	700	$(NdO)_2CO_3$-II + Nd_2O_3-A
	750	NdO_3-A + Nd_2O_3-C
	900	Nd_2O_3-A
(2) $Nd_2(CO_3)_3 \cdot 8H_2O$		
		$Nd_2(CO_3)_3 \cdot 8H_2O$
	90 °C	$Nd_2(CO_3)_3 \cdot 8H_2O$ + $Nd_2(CO_3)_3H_2O$
	150	$Nd_2(CO_3)_3H_2O$
	300	$Nd_2(CO_3)_3$
	413	$Nd_2(CO_3)_3$ + $(NdO)_2CO_3$-I
	430	$(NdO)_2CO_3$-I
	500–530	$(NdO)_2CO_3$-I + $(NdO)_2CO_3$-II
	650	$(NdO)_2CO_3$-II + $(NdO)_2CO_3$-I + Nd_2O_3-C
	at 650	$(NdO)_2CO_3$-II + $(NdO)_2CO_3$-I + Nd_2O_3-C
	at 650 3 hr	Nd_2O_3-C + Nd_2O_3-A
	700	Nd_2O_3-A + Nd_2O_3-C
(3) $Nd_2(CO_3)_3$		
		$Nd_2(CO_3)_3$
	413°C	$Nd_2(CO_3)_3$ + $(NdO)_2CO_3$-I
	424	$(NdO)_2CO_3$-I
	529	$(NdO)_2CO_3$-I + $(NdO)_2CO_3$-II
	600–650	$(NdO)_2CO_3$-II + $(NdO)_2CO_3$-I + Nd_2O_3-C
	700	$(NdO)_2CO_3$-II + Nd_2O_3-C + Nd_2O_3-A
	750	Nd_2O_3-C + Nd_2O_3-A
	850	Nd_2O_3-A + Nd_2O_3-C

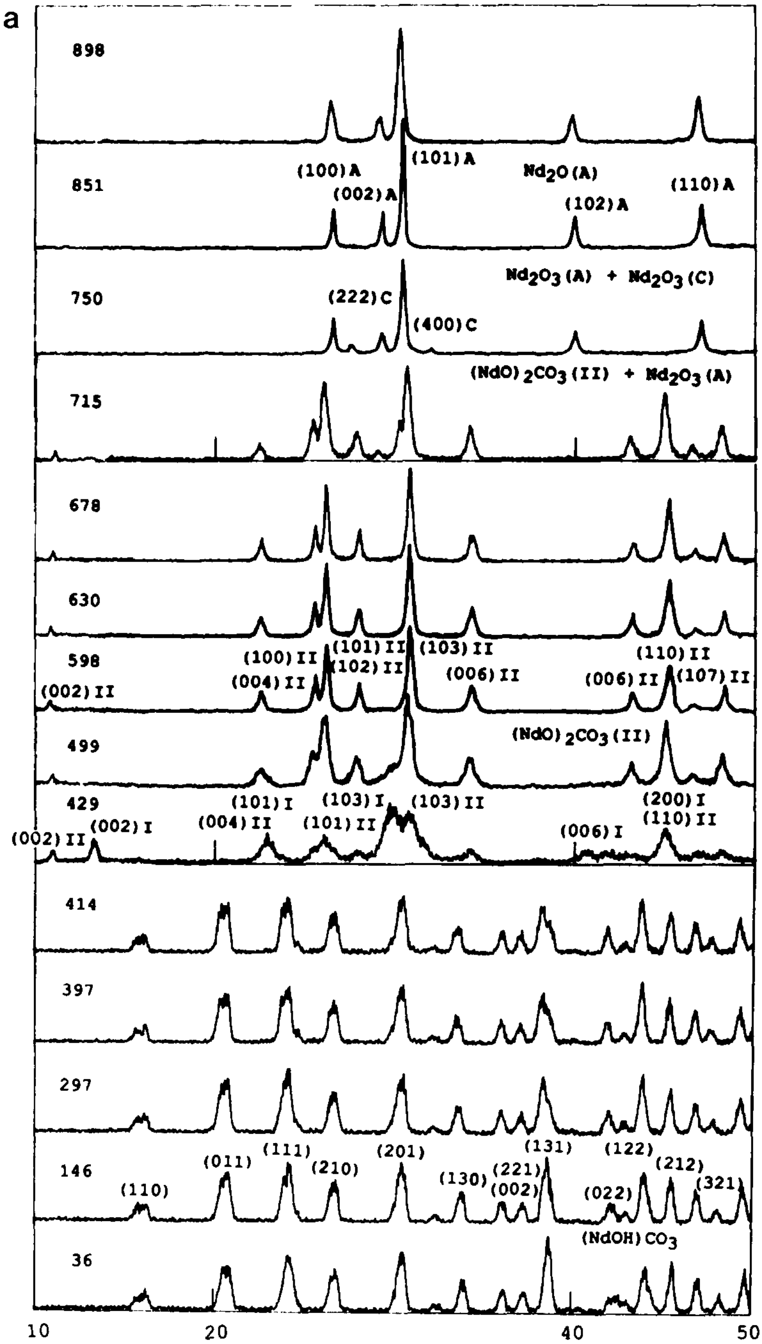

FIG. 3. Sequential high-temperature X-ray diffraction patterns of (a) $NdOHCO_3$ and (b) $Nd_2(CO_3)_3 \cdot 8H_2O$. Temperatures are shown on the left and the decomposition products are identified by the diffraction maxima.

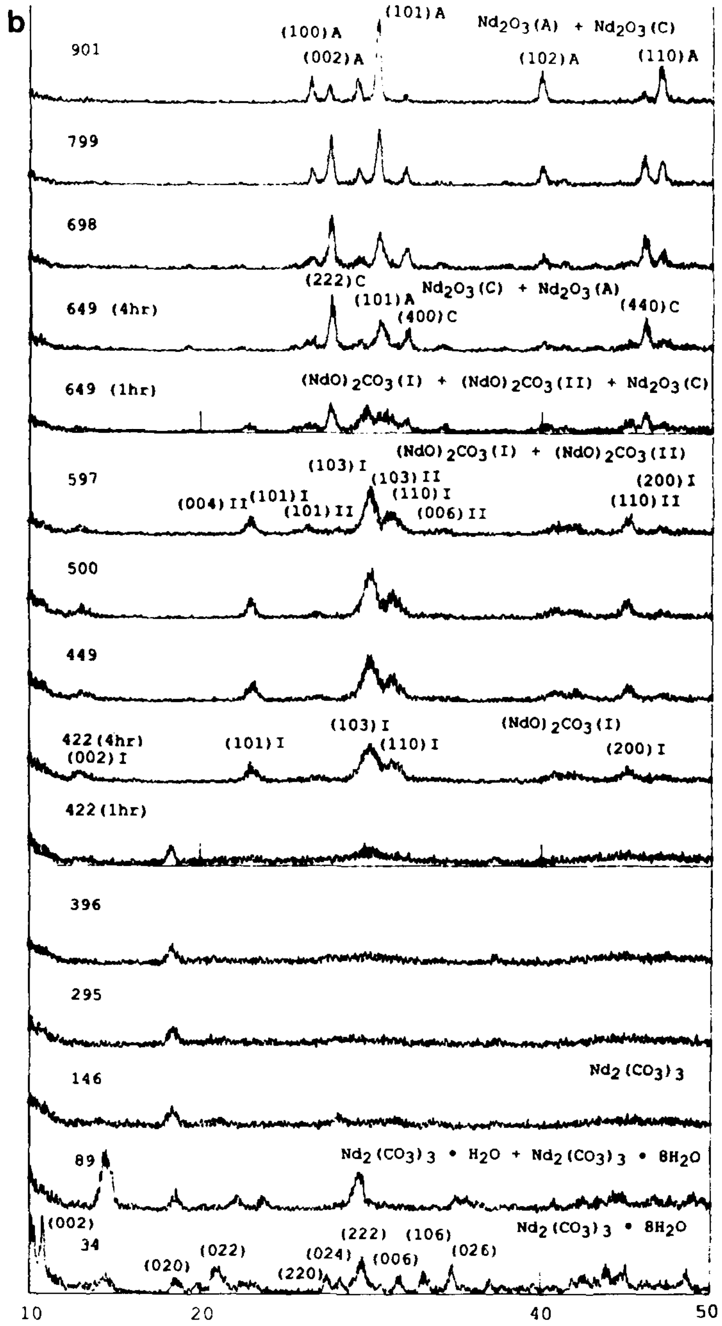

FIG. 3—*Continued*

$NdOHCO_3$ decomposed to $(NdO)_2CO_3$-I and $(NdO)_2CO_3$-II at about 430°C. This decomposition temperature is somewhat higher than that observed in TGA. This is considered to indicate some inaccuracy in the temperature measurement of HTXRD because of a variable packing of the sample powder. A single phase region of type-I was not observed. Type-I $(NdO)_2CO_3$ transformed to type-II at about 600°C. The phase transformation from tetragonal type-I to hexagonal type-II was reported by Turcotte *et al.* (*11*). The type-II was present up to 700°C. This temperature is higher than the starting decomposition temperature of $(NdO)_2CO_3$ determined by TGA (636°C).

The type-II decomposed to Nd_2O_3 (type-A) first at about 700°C. Above this temperature Nd_2O_3 (type-A) and Nd_2O_3 (type-C) are recorded. The existence of the mixture of type-A and type-C is consistent with the powder X-ray diffraction pattern of the TGA sample. Finally only the type-A sesquioxide remained.

(b) The hydrate decomposed in the following sequence:

$$\begin{aligned} &Nd_2(CO_3)_3 \cdot 8H_2O \rightarrow \\ &\quad Nd_2(CO_3)_3 \cdot H_2O \rightarrow Nd_2(CO_3)_3 \rightarrow \\ &\quad (NdO)_2CO_3\text{-I} \rightarrow (NdO)_2CO_3\text{-I} \\ &\quad + (NdO)_2CO_3\text{-II} \rightarrow (NdO)_2CO_3\text{-II} \\ &\quad + (NdO)_2CO_3\text{-I} + Nd_2O_3\text{-C} \rightarrow \\ &\qquad\qquad Nd_2O_3\text{-A} + Nd_2O_3\text{-C}. \end{aligned}$$

The anhydrous $Nd_2(CO_3)_3$ decomposed to type-I first at about 413°C. Type-I was stable up to about 500°C and then started to transform to type-II. The type-C sesquioxide appeared at about 600°C while some type-I still remained. At about 700°C all the dioxymonocarbonate had decomposed to the sesquioxide. The decomposition temperatures are in agreement with those of the TGA method. In one run, a mixture of type-I, type-II, and type-C was present at 650°C for 3 hr, type I and type-II decomposed to type-C and type-A oxides. This result further supports the idea that type-II transforms to type-A. As already described in the TGA section, the decomposition temperature from $(NdO)_2CO_3$ to Nd_2O_3 from $NdOHCO_3$ is somewhat higher than that from $Nd_2(CO_3)_3 \cdot 8H_2O$. The high-temperature X-ray study of $NdOHCO_3$ shows the hexagonal $(NdO)_2CO_3$ decomposing to the oxide Nd_2O_3, and in the decomposition of $Nd_2(CO_3)_3$ the tetragonal $(NdO)_2CO_3$ decomposes to the oxide Nd_2O_3 before the transformation to hexagonal $(NdO)_2CO_3$ is complete. The discrepancy seems to lie in the differences in the stability of tetragonal type-I and hexagonal type-II. Type-II is stable to higher temperatures than type-I. This is also suggested by the work of Turcotte *et al.* (*11*).

Type-A sesquioxide is the decomposition product from $NdOHCO_3$. This decomposition process was reported by Shiffmacher *et al.* (*8*). Type-A transforms to type-C but the final oxide is type-A, suggesting some equilibrium between type-A and type-C. Both the type-II $(NdO)_2CO_3$ and type-A (Nd_2O_3) are structures in which layers of hexagonal (NdO) are separated either by CO_3^{2-} or O^{2-} insertions, so it seems to be easier to decompose from type-II to type-A than from the tetragonal type-I to hexagonal type-A or hexagonal type-II to cubic type-C. In the case of $Nd_2(CO_3)_3$, the first oxide is cubic type-C in coexistence with type-I and type-II. This result indicates that the $(NdO)_2CO_3$-I decomposes to Nd_2O_3-C, and that explains why the $(NdO)_2CO_3$ produced from $Nd_2(CO_3)_3$ during TGA decomposes at lower temperatures than that from $NdOHCO_3$.

From the TGA and HTXRD studies the transformation and decomposition reaction process of $(NdO)_2CO_3$ to Nd_2O_3 is thought to be as follows:

$$\begin{tikzcd} (NdO)_2CO_3\text{-I} \arrow[r] \arrow[d] & Nd_2O_3\text{-C} \arrow[d] \\ (NdO)_2CO_3\text{-II} \arrow[r] & Nd_2O_3\text{-A} \end{tikzcd}$$

(Note that this still leaves unexplained the appearance of C-type Nd_2O_3 at 851° from $NdOHCO_3$.)

(*3*) *High-Resolution Electron Microscopy*

(*a*) *Neodymium hydroxycarbonate* (*α-$NdOHCO_3$*). The decomposition of the α-hydroxycarbonate was investigated utiliz-

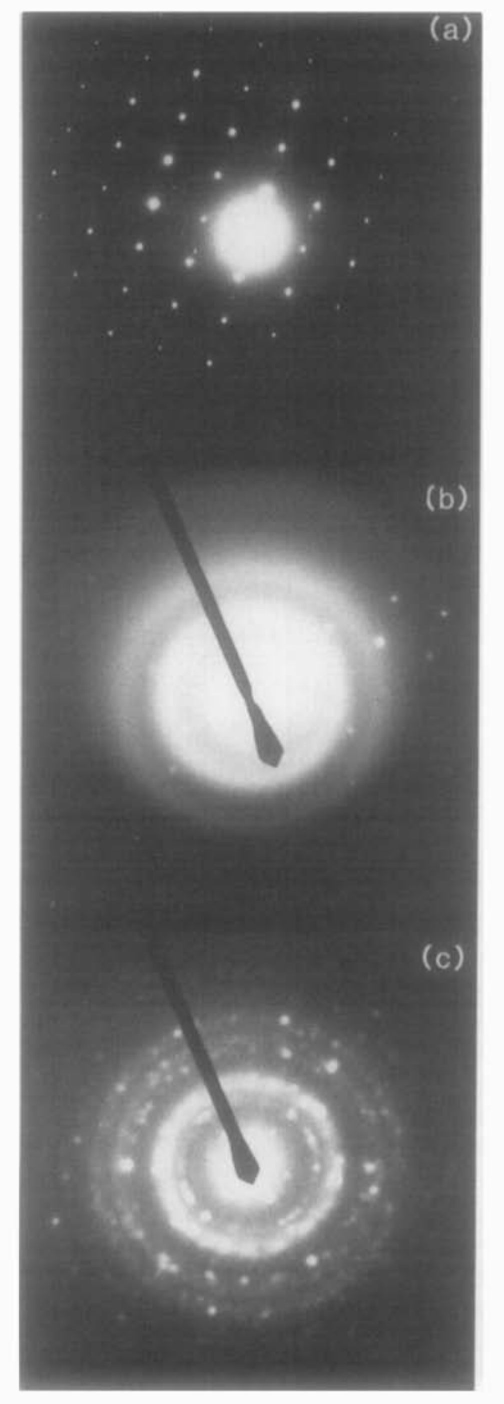

FIG. 4. Electron diffraction patterns of the original sample of (a) α-NdOHCO$_3$, [1$\bar{1}$0] and (b) and (c) where the specimen is transforming to (NdO)$_2$CO$_3$-I.

ing JEOL 200CX and 4000EX microscopes. This compound decomposed rapidly in the 200CX first to an amorphous product out of which the dioxymonocarbonate crystallized. No further decomposition of this specimen was observed.

The sequence of diffraction patterns reproduced in Fig. 4a–c show this sequence clearly. The ordered hydroxycarbonate which yielded the sharp diffraction spots of Fig. 4a changed almost immediately to yield the broad diffuse ring pattern shown in Fig. 4b, characteristic of a very finely divided, poorly crystalline product. Figure 4c records a diffraction pattern of (NdO)$_2$CO$_3$-I. The image at the beginning showed evidence of thin edge nucleation and growth that results in segmented fringes roughly parallel to tangents to the crystal edge. In this sample, consistent with the HTXRD results, a small area of type-II was also observed. The region in which type-I and type-II coexisted was viewed along [020]. In contrast with β-NdOHCO$_3$, α-NdOHCO$_3$ is orthorhombic and has no hexagonal layers of $(\mathrm{NdOH})_n^{2n+}$ (*12, 13*). The $(\mathrm{NdOH})_n^{2n+}$ layers are rearranged to give both type-I and type-II dioxymonocarbonate.

In the 4000EX the hydroxide decomposed completely into the oxide. The hydroxycarbonate rapidly formed a poorly crystalline product. The [020] diffraction pattern of α-NdOHCO$_3$ (Fig. 5a) immediately changed to a diffuse ring pattern that was identified as a mixture of type-I and type-II (Fig. 5b).

Figure 6a shows a region of the coexistence of type-II, type-C, and type-A. Figures 6b to e show the optical diffraction patterns corresponding to the areas 1–4 in Fig. 6a. Figure 6b corresponds to the type-II (0001) spacing, and Fig. 6c is type-C (222). And also Fig. 6 shows the type-A (002) spacing. The direction of (002) type-II and (222) type-C is the same. The type-C oxide has a cubic structure and the [111] cubic direction corresponds to [0001] hexagonal.

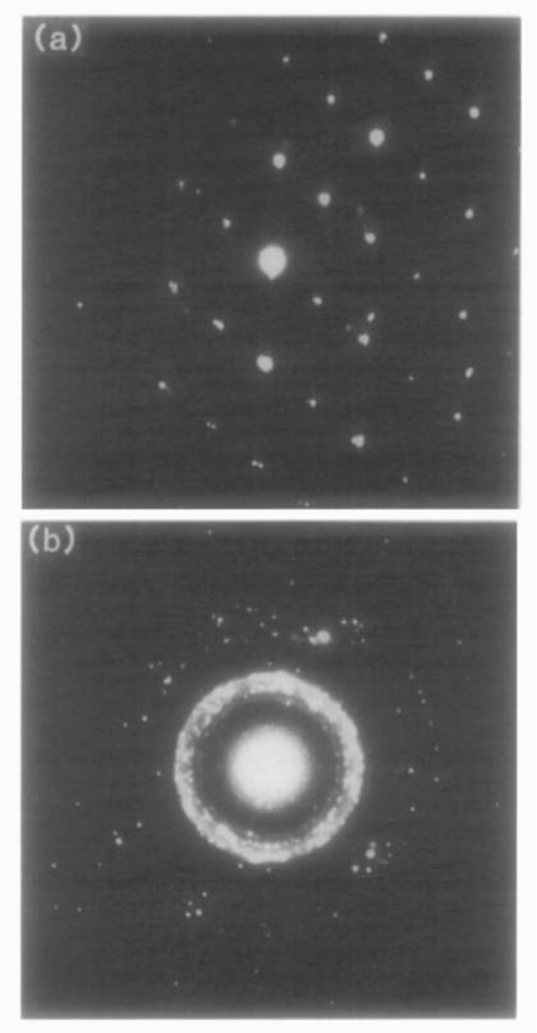

FIG. 5. Electron diffraction patterns of (a) α-$NdOHCO_3$ [020] and (b) types I and II $(NdO)_2CO_3$ decomposition products.

So the epitaxial relationship among type-II, type-C, and type-A is [002]II//[111]C//[002]A. These directions are perpendicular to the $(NdO)_n^{n+}$ layers.

Comparing areas 2, 3, and 4, as mentioned above, an epitaxial relationship between type-A and type-C exists as [002]A//[222]C. The images show that type-C transforms to type-A or that type-A goes to type-C. We could not observe directly a clear indication of this transformation in a specific area. Furthermore, there is no direct information about the transformation between type-I and type-C. However, considering the results of HTXRD and the decomposition of $Nd_2(CO_3)_3$, we believe that type-C transforms to type-A and that the epitaxial relationship is [002]A//[222]C.

Figure 7a shows an image of another area with some marked areas of optical diffraction. Figures 7b–f show optical diffraction patterns of areas 1–5, respectively, in Fig. 7a. In the area of Fig. 7c, [4-40] of type-C and [020] of type-A coexist, so the same epitaxial relationship is observed as in Fig. 6.

For α-$NdOHCO_3$, using the results of high-temperature X-ray observation and those of HREM, the decomposition process is summarized as follows:

$$\begin{tikzcd} \alpha\text{-NdOHCO}_3 \arrow[r] & (\text{NdO})_2\text{CO}_3\text{-I} \arrow[r] \arrow[d] & \text{Nd}_2\text{O}_3\text{-C} \arrow[r] & \text{Nd}_2\text{O}_3\text{-A} \\ & (\text{NdO})_2\text{CO}_3\text{-II} \arrow[urr] & & \end{tikzcd}$$

(*b*) *Neodymium Carbonate Anhydrate* (*$Nd_2(CO_3)_3$*). $Nd_2(CO_3)_3$ was introduced into the JEOL 4000EX electron microscope as a poorly crystalline sample. The initial electron diffraction pattern is shown in Fig. 8. In the decomposition of the anhydrous carbonate it was possible to record on film and on videotape the violent processes of the decomposition with the loss of CO_2 gas and recrystallization. For example, in Fig. 9 the tetragonal, type-I dioxymonocarbonate (identified from the electron diffraction pattern and optical diffraction pattern of the image) is observed to nucleate and grow crystalline structures from the thin edge inward (a similar process was observed in the decomposition of $Nd_2(CO_3)_3 \cdot 8H_2O$ and $NdOHCO_3$, beam current = 9 A/cm^2 with a time interval between exposures of 1 min). The first decomposition of the carbonate is type-I alone. This result agrees

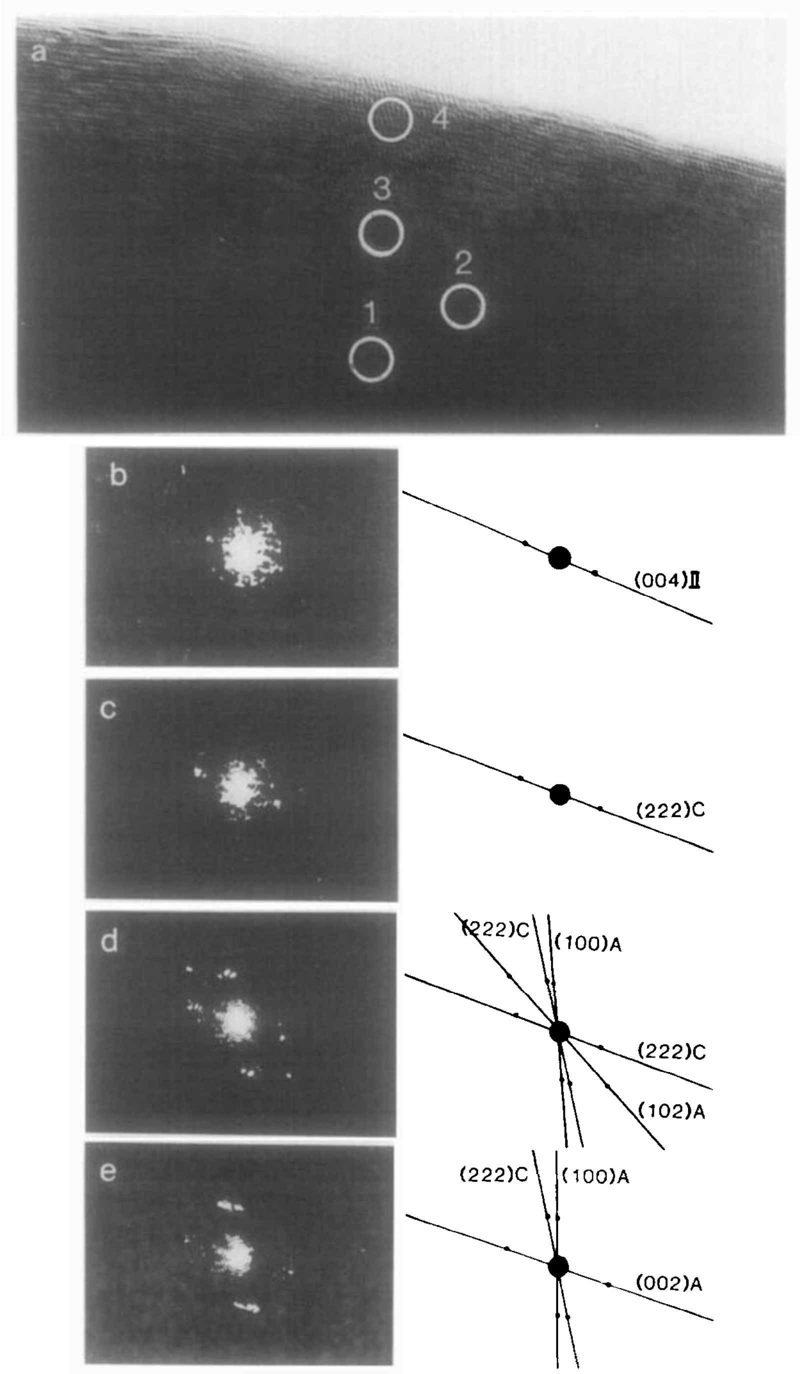

FIG. 6. (a) A fringe image of the decomposition products from α-$NdOHCO_3$. (b)–(e) Optical diffraction patterns and their analyses of the regions marked 1–4 in image (a).

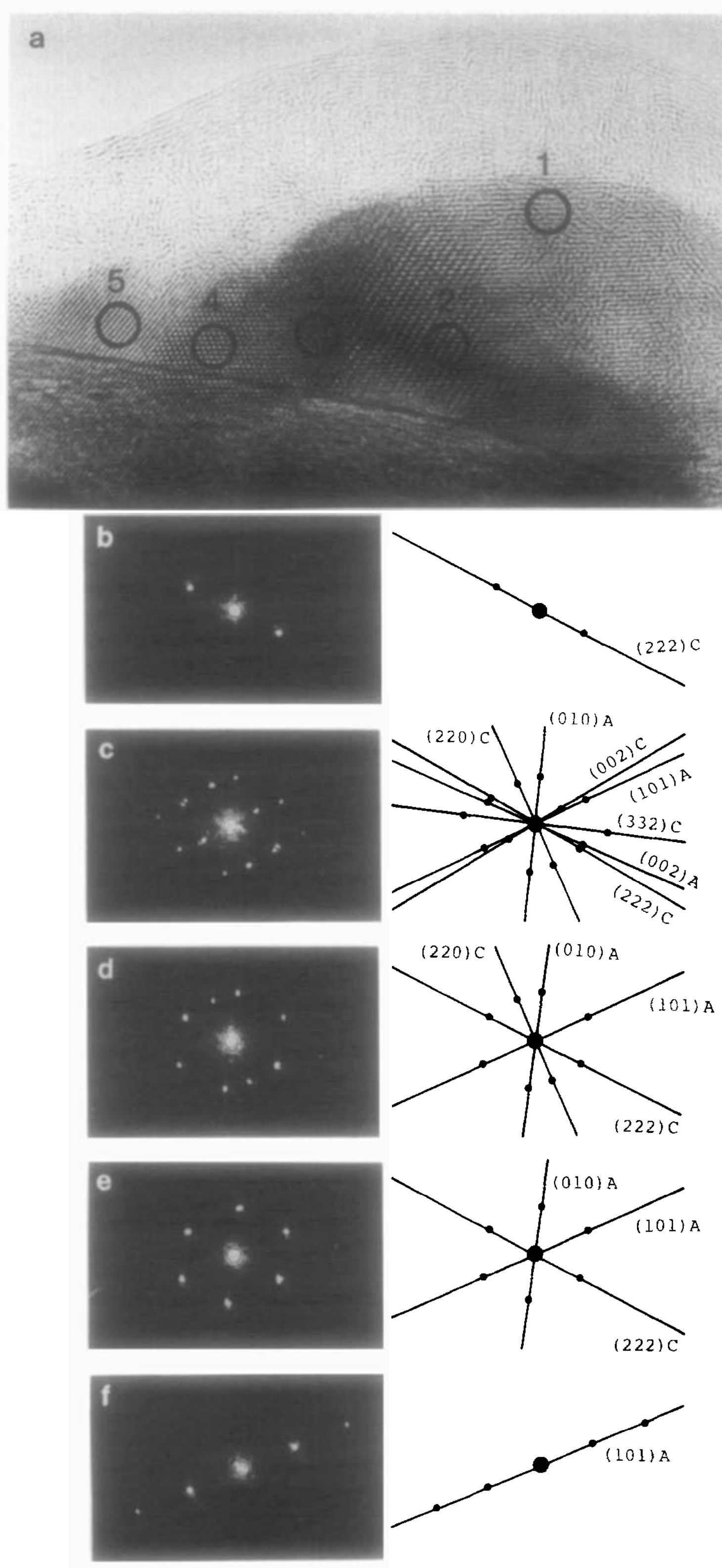

FIG. 7. (a) An image of the decomposition products from α-$NdOHCO_3$. (b)–(f) Optical diffraction patterns and their analyses of regions marked 1–5 in image (a).

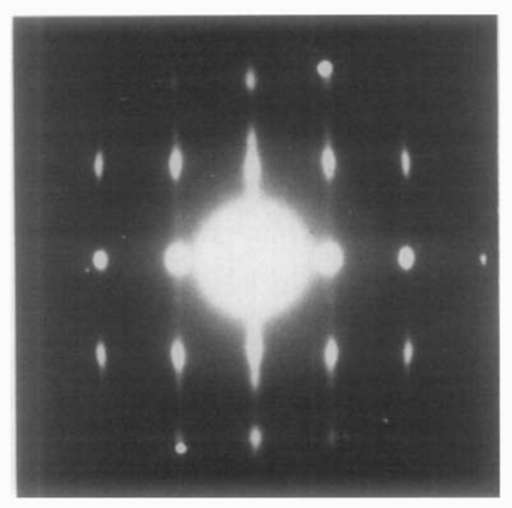

FIG. 8. An electron diffraction pattern of the $Nd_2(CO_3)_3$ immediately after it was introduced into the microscope.

well with that of the high-temperature X-ray method.

The reaction in which type-II decomposes to Nd_2O_3-A was accompanied by violent upheavals followed by faceting and recrystallization as suggested in Fig. 10. The time interval between (a) and (b) is 16 min (2 min of beam current at 30 A/cm^2 and the rest of the time at 9 A/cm^2). Figure 10a is an image of a highly faulted $(NdO)_2CO_3$-II. In Fig. 10b, the formation of Nd_2O_3-A is clearly shown in the thin edge as the specimen reconstructs during the loss of CO_2. As the reaction subsided it was possible to record on videotape the late stages of CO_2 loss from the edge as the oxide formed. The videorecording emphasizes the explosive vigor of the process even in the last stages. This sequence of images reveals that the dioxymonocarbonate type-II decomposes to the sesquioxide type-A. Figure 11 shows the final product, A-type Nd_2O_3, that has grown into a quite large domain.

In the microscopic observation of the decomposition of the hydroxycarbonate, only the transformation of type-II to type-A was observed. No evidence of transformation of type-I to type-II or type-I to type-C was found.

(*c*) *Neodymium Carbonate Octahydrate* (*$Nd_2(CO_3)_3 \cdot 8H_2O$*). $Nd_2(CO_3)_3 \cdot 8H_2O$ decomposed rapidly in the electron beam of the JEOL 4000EX. Apparently the short diffusion path of CO_2 in the thinnest edge allows the first nucleation of type-I dioxy-

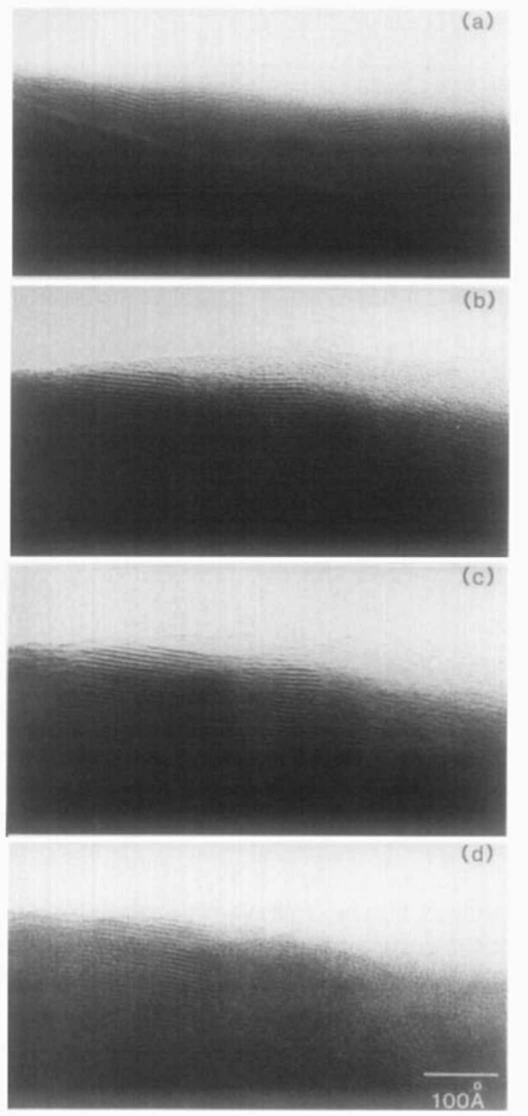

FIG. 9. Fringe images of $(NdO)_2CO_3$-I produced from $Nd_2(CO_3)_3$. The sequential images were taken at after 1- and 3-min intervals. Note the development of order from the edge inward.

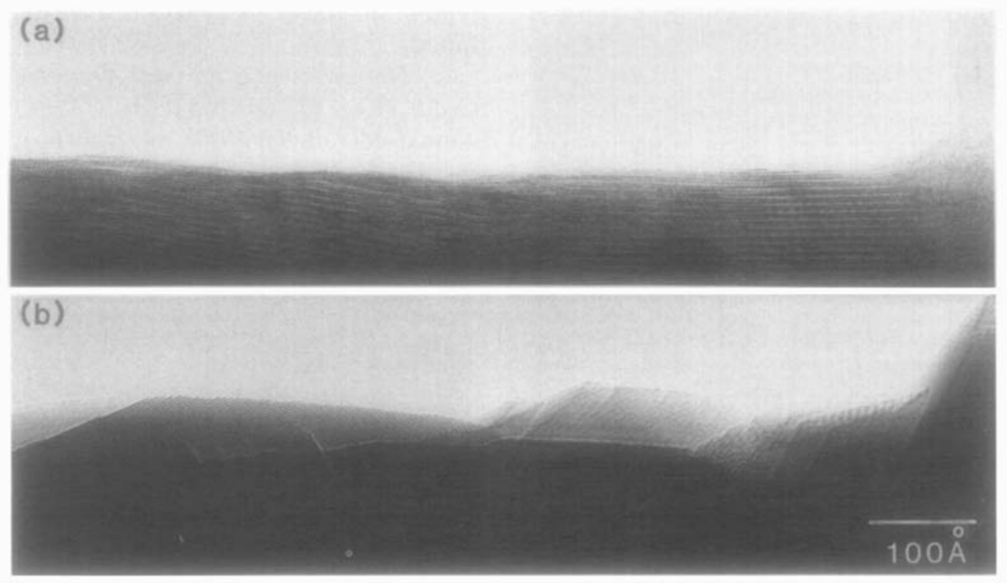

FIG. 10. A profile image of $(NdO)_2CO_3$-II. (a) During decomposition to A-type Nd_2O_3 and (b) as CO_2 is eliminated.

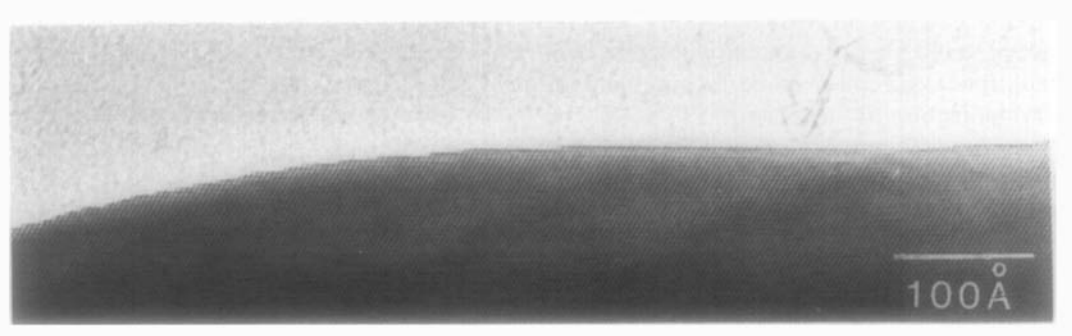

FIG. 11. A structure image of A-type Nd_2O_3 [001] which is the final product of the decomposition of $Nd_2(CO_3)_3 \cdot 8H_2O$.

monocarbonate followed by impingement of the growing domains. The domains crystallize tangentially at the curved edge producing segmented patterns with mismatched interfaces. No further decomposition of this specimen was observed.

Acknowledgments

It is a pleasure to acknowledge major support from NSF Grant DMR-8516381 and to NSF Grant DMR-8611609 for making the high-resolution electron microscopic facilities available.

References

1. E. L. HEAD AND C. H. HOLLEY, JR., *in* "Rare Earth Research II" (K. Vorres, Ed.), Vol. 2, p. 51, Gordon & Breach, New York (1964).
2. M. AKINC AND D. SORDELET, *Adv. Ceram. Mater.* **2,** 232 (1987).
3. R. L. N. SASTRY, S. R. YOGANNRASIMHAN, P. N. MEHROTRA, AND C. N. R. RAO, *J. Inorg. Nucl. Chem.* **28,** 1165 (1966).

4. W. W. Wendlandt and T. D. George, *Texas J. Sci.* **13,** 316 (1961).
5. R. G. Charles, *J. Inorg. Nucl. Chem.* **27,** 1489 (1965).
6. Tiao-Han Cheng and Mei-wan Yen, *T'ai-wan K'o Hsueh* **30,** 137 (1976).
7. H. Dexpert, G. Shiffmacher, and P. Caro, *J. Solid State Chem.* **15,** 301 (1975).
8. G. Schiffmacher, H. Dexpert, and P. Caro, *in* "Reactivity of Solids," Proceedings, Int. Symp., 8th Meeting, 641 (1976).
9. M. L. Salusky and L. L. Quill, *J. Amer. Chem. Soc.* **72,** 3306 (1950).
10. J. O. Sawyer, P. Caro, and L. Eyring, *Monatsh. Chem.* **102,** 333 (1971).
11. R. P. Turcotte, J. O. Sawyer, and L. Eyring, *Inorg. Chem.* **8,** 236 (1969).
12. J. O. Sawyer, P. Caro, and L. Eyring, *Rev. Chim. Miner.* **10,** 93 (1973).
13. H. Dexpert and P. Caro, *Mater. Res. Bull.*, 9, 1577 (1974).